arXiv:1603.06175v6 [physics.soc-ph] 9 Sep 2016

Dynamical capacity drop in a nonlinear stochastic traffic model

Wei-Liang Qian[1,2], Adriano F. Siqueira[1], Romuel F. Machado[3], Kai Lin[4] and Ted William Grant[1]

[1] *Escola de Engenharia de Lorena, Universidade de São Paulo, SP, Brasil*

[2] *Faculdade de Engenharia de Guaratinguetá, Universidade Estadual Paulista, SP, Brasil*

[3] *Instituto de Ciências Exatas e Biologicas, Universidade Federal de Ouro Preto, SP, Brasil and*

[4] *Instituto de Física e Química, Universidade Federal de Itajubá, MG, Brasil*

(Dated: September 13, 2016)

In this work, we show that the inverse-λ shape in the fundamental diagram of traffic flow can be produced dynamically by a nonlinear mesoscopic model. The key features in the fundamental diagram are shown to be closely related to the properties of the stochastic equation of motion as well as the stochastic stabilities of the steady and quasi-stationary solutions. In our model, the scattering of the data is attributed to the noise terms introduced in the stochastic differential equations; while the inverse-λ shape and the associated sudden jump of physical quantities arise, due to the effect of stochastic noises on the stability of the system. The model parameters are calibrated and compared qualitatively with the data.

INTRODUCTION

Based on the empirical observations accumulated on highways in different countries for nearly 8 decades (see for instance ref.[1–4]), one important empirical feature of the so called "fundamental diagram" of traffic flow is the inverse-λ shape [5–8] accompanying with capacity drop [9–11]. The inverse-λ implies discontinuity of the flow as a function of vehicle density which occurs close to the maximum of the flow. Consequently the flow-concentration curve is divided into two different regions of lower and higher vehicle density respectively, known as "free" and "congested" flow. However, the recent data analysis [4, 12, 13] gives birth to an intriguingly different viewpoint. When one divides the empirically observed data into stationary and non-stationary traffic conditions, the resulting fundamental diagram is continuous and scatter-free when one is only interested in the *average values* of sustained periods of nearly *stationary* traffic conditions. In [4], each point in the scatterplot in question corresponds to the average properties of prolonged periods ($\sim$ 10 min) of near-stationary traffic states. It exhibits a well-defined relation between flow and concentration, which does not show evidence of discontinuities. The scatterplot obtained from the near-stationary data is understood to be different from that obtained by simply collecting consecutive time intervals of fixed duration. The latter includes the information of non-stationary states, which mostly capture the scattering feature of the data points. In particular, if one plots the flow and concentration data measured over smaller aggregation interval ($\sim$ 2 min), both the discontinuity and the scattering nature of the data reappear. While the discontinuity measures the difference between free and congested traffic states, the observed scatter is associated to the non-stationary transitions between the two traffic states. Therefore, a part of the observed complexity in the fundamental diagram could be understood as a result of mixing (averaging) traffic data from stationary and non-stationary traffic conditions. The above analysis and the train of thought are well recognized and adopted by many authors [14–23]. In particular, the observation of the so called "macroscopic fundamental diagram" [22, 23] aroused much interest follows the very same line of thought. In recent years, further developments including new methods and models were proposed, and debate continues as how to address the scatter [24, 25], and the capacity drop [16, 17].

In this work, we attempt to show that both the inverse-λ shape and its dissapearance can be understood within a nonlinear stochastic model. As it will be shown below, for near-stationary traffic states, observable traffic states corresponds to stable solutions of the deterministic equation of motion, and the resultant fundamental diagram is continuous and the deviation is small; for non-stationary traffic states, on the other hand, random noises modify stability of the corresponding stochastic equation of motion, and the resulting fundamental diagram becomes discontinuous and shows a inverse-λ shape. We note that a key characteristic of the present approach concerns how to model the randomness in traffic flow. From an empirical viewpoint, the uncertainties observed in the data can be always expressed in terms of the variance of the fundamental diagram, which has become an intriguing topic in recent years [26–30]. To study such uncertainties, methodologies involving stochastic modeling have aroused much attention, either from macroscopic viewpoint [31–34], from microscopic models [35–44] or from phenomenological approaches [45–47]. On the one hand, even under stationary traffic conditions, certain degree of residual scatter always persists. They are, for the most part, statistical in nature. The cause of such uncertainty can be attributed to heterogeneous drivers [48] and lane changes [49] among others. On the other hand, when the fundamental diagram is obtained by using a smaller

aggregation interval, it may carry the information on the intrinsically non-stationary state or the dynamics of transitions between different traffic states. These non-stationary states can be either deterministic or stochastic. In literature, many parsimonious models were developed in their efforts to understand the underlying dynamics. Some of these traffic conditions are understood to be connected to the instability of the equation of motion [50–54] associated to phase transitions (bifurcations) in the system [44, 55–58], or to social dilemma structures where a fair Pareto optimum (the best solution for all) is not necessarily consistent with the best solution for individuals [59]. The scatter of the data can be either attributed to the (transient) temporal evolution of the dynamical system (such as stop-and-go wave [50, 60–65]), or to the "synchronized flow" defined in the three phase traffic theory [66, 67].

Our model is based on a mesoscopic approach considering discrete speed states. It makes use of the stochastic differential equations (SDE) to model the system with stochastic noises. Our claim is that the sudden jump can be explained in terms of the modified stability of the system due to the stochastic noises. In what follows, we firstly present a simplified deterministic models characterized by the "fold" catastrophe potential functions. It is shown that the model leads to two different traffic phases, and the two phases joins continuously at the transition point with maximum flow. Secondly, the model is generalized to include stochastic nature. We investigate numerically the stability of the solutions of the SDE and study the variance of the flow. It turns out that the appearance of the discontinuity in the fundamental diagram is obtained naturally without introducing any additional free parameters. The present model is then compared qualitatively to the data from I-80 freeway collected under the NGSIM program. Conclusion remarks and perspectives are given by the end of the paper.

A MESOSCOPIC "FOLD CATASTROPHE" MODEL

In this section, we introduce a nonlinear mesoscopic model with minimal number of parameters which provides analytic solution for two traffic states, namely, free flow state and congested flow state. We also show this model is equivalent to a fold catastrophe model. The non-linear model can been viewed as a generalization of a mesoscopic traffic model [68] proposed recently. In the ref [68] one only considers linear cases and the stability of the stationary solutions were not investigated. However, it is widely known that traffic congestion is caused by the instability of the system; therefore it is essential to generalize the model into the nonlinear domain and explicitly study the stability of the stationary solutions. As shown below, not all solutions are globally stable, and only stable solutions and quasi-stationary solutions can be associated to observable traffic states. Following our recent studies [68, 69] [1], let us consider a section of one-lane highway of length L and with two speed states $v_1 < v_2$. Also one assumes that the total vehicle number N is conserved. The equation of motion (EoM) of the model is essentially a simplified transport equation given by

$$\begin{aligned} \frac{dn_1}{dt} &= -c_1 n_1 + c_2 n_1 n_2 \frac{1}{N_{max} - N} \\ \frac{dn_2}{dt} &= -c_2 n_2 n_1 \frac{1}{N_{max} - N} + c_1 n_1 \end{aligned} \tag{1}$$

[1] A preliminary version of the model can be found in [70].

where n_i $(i = 1, 2)$ is the occupation number of corresponding velocity state v_i and N_{max} is maximal congestion number owing to finite vehicle size. So $k_{max} = N_{max}/L$ is the corresponding maximal vehicle density leading to complete congestion. The physical contents of the equation and of the coefficients are the following. The transition rate of n_1 is determined by the r.h.s. of the equation consisting of a loss term and a gain term. The loss term $c_1 n_1$ is simply proportional to the occupation number since cautious slow drivers leave this state at a fix rate. In addition of being proportional to n_2, the gain term must also be proportional to n_1, since slow drivers force the fast ones to slow down to their velocities. The extra constant factor $\frac{1}{N_{max}-N}$ takes the total congestion into account as explained below. It is easy to show that Eq.(1) guarantees the total vehicle conservation $N = n_1 + n_2$ and hence there is only one degree of freedom. Therefore one may simply consider the following equation in terms of n_1.

$$\frac{dn_1}{dt} \equiv f(n_1) = -c_1 n_1 + c_2 n_1 \frac{N - n_1}{N_{max} - N} \tag{2}$$

Its stationary solution n^* is given by setting the r.h.s. of the above equation to zero:

$$-c_1 n_1 + c_2 n_1 \frac{N - n_1}{N_{max} - N} = 0 \tag{3}$$

and one obtains

$$n_f^* = 0 \tag{4}$$

or

$$n_g^* = N - \frac{c_1}{c_2}(N_{max} - N) \tag{5}$$

These solutions are stable against small deviations if the stability criterion [69]

$$\frac{df}{dn_1}(n_{f,g}^*) = -c_1 + (c_2 N - 2c_2 n_{f,g}^*)\frac{1}{N_{max} - N} < 0. \tag{6}$$

is satisfied. So the null solution n_f^* is stable for $N < \frac{c_1}{c_1+c_2} N_{max}$ while the non-null n_g^* is stable for $N > \frac{c_1}{c_1+c_2} N_{max}$. It can be inferred from Eq.(9) (as well as from Fig.1) below that n_f^* corresponds to free flow solution while n_g^* is related to the congested flow solution. Since $\frac{c_1}{c_1+c_2} N_{max}$ plays the role of a critical density, we will introduce the parameter N_c given by

$$N_c = \frac{c_1}{c_1 + c_2} N_{max} \tag{7}$$

With two speed states the flux is given by

$$q = k\frac{n_1 v_1 + n_2 v_2}{N} = \frac{1}{L}(n_1 v_1 + n_2 v_2) \tag{8}$$

where the vehicle density $k = N/L$. This model predicts two distinct behaviors for the flux q, namely

$$q = \begin{cases} q_{free} = k v_2 & N \le N_c \\ q_{congested} = q_c + \left[v_1 - \frac{c_1}{c_2}(v_2 - v_1)\right](k - k_c) & N_c < N \le N_{max} \end{cases} \tag{9}$$

where $k_c = N_c/L$ and $q_c = k_c v_2$. The fundamental diagram in this case is a *continuous* curve made up of two straight lines with inclinations v_2 and $v_1 - \frac{c_1}{c_2}(v_2 - v_1)$. A schematic fundamental diagram for $v_1 = 0.0$ is shown in the top left panel of Fig.1, and the corresponding curve of average velocity vs. vehicle density is shown in the bottom left panel. One sees that the flow arises linearly in the free flow phase $N < N_c$ and hits its peak at $N = N_c$, then the system switches to the second stationary solution while the flow drops linearly until it vanishes while attaining $k = k_{max}$. The average velocity remains as a constant in the free flow phase and it starts to drop linearly at $N = N_c$ until hitting zero at complete congestion. Let it be noted that these solutions are exact.

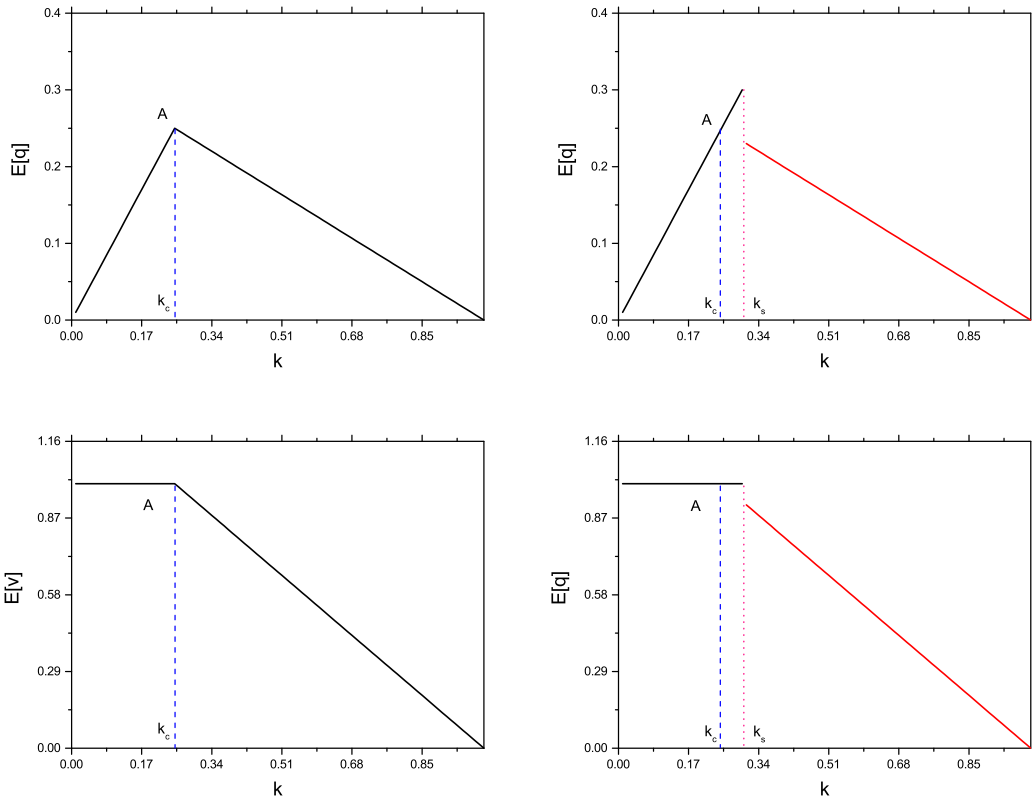

FIG. 1. Schematic results from the two-speed-state model when the following trivial parametrization were adopted $v_1 = 0$, $v_2 = c_1 = N_{max} = 1$, $c_2 = 3$. Top left: The fundamental diagram without stochastic noises. Top right: The fundamental diagram when stochastic noises are considered. Bottom left: The average velocity as a function with vehicle density without stochastic noises. Bottom right: The same as the bottom left plot but with the presence of stochastic noises. The location of k_s is illustrative.

It is not difficult to show that the above simple model is equivalent to a "fold catastrophe" model [71], with the minima of its potential function being the same as the roots of Eq.(3). The fold potential function is a third order polynomial:

$$V(n_1)^{(fold)} = \frac{1}{3}\frac{1}{N_{max} - N}c_2 n_1^3 + \frac{1}{2}(c_1 - \frac{1}{N_{max} - N}c_2 N)n_1^2 \tag{10}$$

where the stable stationary state corresponds to its minima.

A STOCHASTIC "FOLD CATASTROPHE" MODEL

Up to this point, we have not considered the effect of stochastic transition terms. The physical content of these transitions is closely related to the stochastic nature of traffic system and therefore may partly provide a mathematical implementation for the "scattering nature" of fundamental diagram. In addition, as we are about to show in this section, the introduction of stochastic noises may modify the stability of stationary solution of the "fold catastrophe" model. As a result, the fundamental diagram is affected. It becomes discontinuous and an inverse-λ shape appears near the maximum of the flow. In our approach, the stochastic noises are studied by making use of SDE. Let us introduce stochastic noises into the above "fold catastrophe" model as following

$$\begin{aligned} dn_1 &= \left(-c_1 n_1 + c_2 n_1 n_2 \frac{1}{N_{max} - N}\right) dt - \alpha\sqrt{c_1 n_1} dB_1 + \alpha\sqrt{\frac{c_2 n_1 n_2}{N_{max} - N}} dB_2 \\ dn_2 &= \left(-c_2 n_2 n_1 \frac{1}{N_{max} - N} + c_1 n_1\right) dt - \alpha\sqrt{\frac{c_2 n_2 n_1}{N_{max} - N}} dB_2 + \alpha\sqrt{c_1 n_1} dB_1 \end{aligned} \tag{11}$$

where B_1 and B_2 are independent Brownian motions and Itô formulas [72] are assumed. The parameter α measures the strength of the stochastic noise: for $\alpha = 0$, the model reduces to the deterministic counterpart. In the this section, we restrict ourselves to the case $\alpha = 1$.

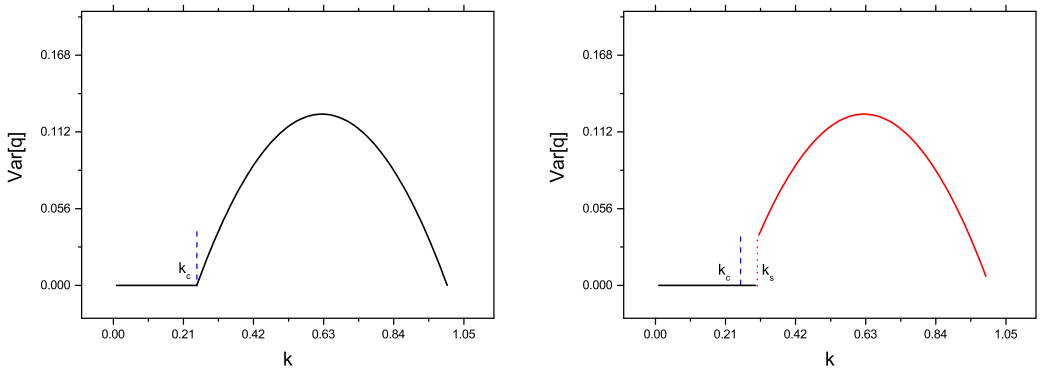

FIG. 2. Schematic variance of the fundamental diagram of the "fold catastrophe" model. In the calculation, one uses the same trivial parameters in Fig.1 $v_1 = 0$, $v_2 = c_1 = N_{max} = L = 1$, $c_2 = 3$. In the left panel, the curves show the variances determined by Eq.(18); in the right panel, stochastic stability of the solutions are considered, the congested flow state shrinks while free flow state extends to k_s. The location of k_s is illustrative.

To evaluate the expected value, it is mathematically rigorous to ignore the stochastic transition terms, when the coefficient of the stochastic transition terms (such as $\alpha\sqrt{c_1 n_1}$ for instance) $\in \mathcal{V}$ (see Theorem 3.2.1 of [72] for the definition of $\mathcal{V}$, which is satisfied for most well behaved functions). One is then left to determine whether these stationary solutions are indeed stochastically stable. However, to the best of our knowledge, to obtain any analytic result on the stability of SDE is not an easy task [73–76]. In Appedix I, we show analytically that for $N < N_c$, the free flow solution in Eq.(9) for deterministic equation (Eq.(1)) is indeed stable for the corresponding SDE (Eq.(11)). For other values of N, numerical studies are carried out to determine the stability of the stable solutions. The results are presented in

Appendix II. It turns out that the SDE possesses different stability properties comparing to the corresponding deterministic EoM. It is found that the free flow solution is stochastically stable within the range $0 < N < N_s$ where the value N_s is numerically found to be bigger than N_c. When $N \geq N_s$, the system dwells around a quasi-stationary solution [77] for a very long period until it eventually evolves to the absorbing boundary[2]. Therefore, we interpret the quasi-stationary solution in the region $N_s < N < N_{max}$ in our model as the congested flow.

For stable solution, one calculates the variance of expected value following the standard procedure of Itô calculus. It is not difficult to show that the variances of the flow reads

$$d(n_1^2) = \left[-2c_1 n_1^2 + 2c_2 n_1^2 \frac{N - n_1}{N_{max} - N}\right] dt + c_1 n_1 dt + c_2 n_1 \frac{N - n_1}{N_{max} - N} dt \tag{12}$$

$$- 2\sqrt{c_1 n_1^3} dB_1 + 2\sqrt{c_2 n_1^3 \frac{(N - n_1)}{N_{max} - N}} dB_2 \tag{13}$$

where one made use of $d(n_1^2) = 2n_1 dn_1 + (dn_1)^2$. For steady state, one has

$$\left[-2c_1 + 2c_2 \frac{N}{N_{max} - N} - c_2 \frac{1}{N_{max} - N}\right] \mathrm{E}[n_1^2] - 2c_2 \frac{1}{N_{max} - N} \mathrm{E}[n_1^3] + \left[c_1 + c_2 \frac{N}{N_{max} - N}\right] \mathrm{E}[n_1] = 0 \tag{14}$$

In principle, one should further evaluate $d(n_1^3)$, which turns out to depend on higher order terms. For simplicity, we approximate the equation chain by ignoring higher order correlation and thus assuming $\mathrm{E}[n_1^3] \sim \mathrm{E}[n_1]\mathrm{E}[n_1^2]$. This cuts the infinite equation chain at second order and obtains

$$\mathrm{E}[n_1^2] = \frac{\left[c_1 + c_2 \frac{N}{N_{max} - N}\right] \mathrm{E}[n_1]}{2c_1 - c_2 \frac{N}{N_{max} - N} + 2c_2 \frac{1}{N_{max} - N} \mathrm{E}[n_1]} \tag{15}$$

Therefore, we approximately have

$$\begin{aligned} \mathrm{Var}[n_1] = \mathrm{Var}[n_2] &= -\mathrm{Cov}[n_1 n_2] \\ &= \frac{\left[c_1 + c_2 \frac{N}{N_{max} - N}\right] \mathrm{E}[n_1]}{2c_1 - 2c_2 \frac{N}{N_{max} - N} + c_2 \frac{1}{N_{max} - N} + 2c_2 \frac{1}{N_{max} - N} \mathrm{E}[n_1]} - \mathrm{E}[n_1]^2 \end{aligned} \tag{16}$$

And the corresponding variance of the flow reads

$$\mathrm{Var}[q] = \frac{(v_2 - v_1)^2}{L^2} \left\{ \frac{\left[c_1 + c_2 \frac{k}{k_{max} - k}\right] \mathrm{E}[n_1]}{2c_1 - 2c_2 \frac{k}{k_{max} - k} + c_2 \frac{1}{L(k_{max} - k)} + 2c_2 \frac{1}{L(k_{max} - k)} \mathrm{E}[n_1]} - \mathrm{E}[n_1]^2 \right\} \tag{17}$$

By making use of Eq.(9), it can be simplified to the following form

$$\mathrm{Var}[q] = \begin{cases} 0 & N \leq N_c \\ 2(v_2 - v_1)^2 \frac{c_1}{c_2} \left(\frac{c_1}{c_2} + 1\right) (k - k_c)(k - k_{max}) & N_c < N \leq N_{max} \end{cases} \tag{18}$$

[2] A type of boundary for the Fokker-Planck equation with the property that once the system evolves to it, it never comes back. It can be easily shown that $n_1 = 0$ is a absorbing boundary in the present problem [77].

We note that the appearance of N_s breaks the continuity of the fundamental diagram. The free flow solution does not stop at N_c (where it intersects with the congested flow solution at point "A" in the left panel of Fig.1) but continues until N_s. Correspondingly, the congested flow solution appears as a quasi-stationary solution only when the concentrations are bigger than N_s, which causes a gap, $\Delta q = q_{free}(N_s) - q_{congested}(N_s)$, at N_s, as can be inferred from Eq.(9).

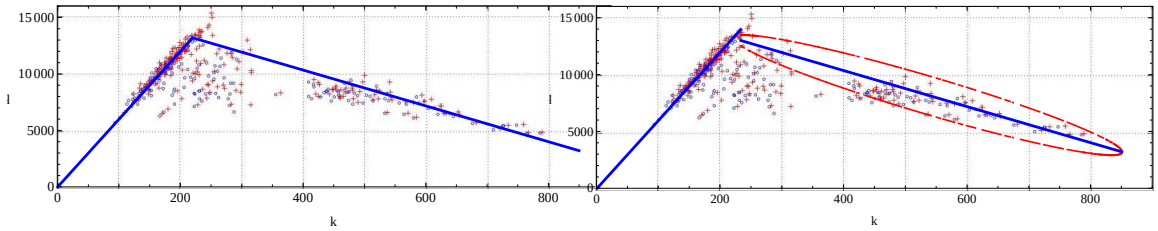

FIG. 3. Fit of the model together with the data from I-80 freeway collected under the NGSIM program. The blue lines are the fit for the average flow while the dotted red lines enclose its standard deviation. The scatterplot is from ref.[78]. The fit was obtained by using the following parameters: $k_{max} = 850, v_1 = 0.37, v_2 = 6, L = 10.0, c_1/c_2 = 0.35$. The left panel shows the fit for the deterministic "fold catastrophe" model, the right panel presents that for the stochastic "fold catastrophe" model where a small gap accompanying by the inverse-λ shape appears due to the stochastic noises.

In Fig.2, we present the schematic results of the variation of the fundamental diagram by using the same parameters as those in Fig.1. It is shown that the variance is zero in the free flow phase due to fact that $\mathrm{E}[n_1] = 0$. Then the variance increases when the system enters congested phase (as an unstable solution at first when $N_c < N < N_s$). It reaches the maximum and eventually decreases to zero when the complete congestion occurs, as seen from Eq.(18). A qualitative comparison to the data is shown in Fig.3. As shown in the left panel of Fig.3, for the deterministic "fold catastrophe" model, the maximum of the flow occurs at $N = N_c$ which corresponds to the tip of the triangle of the left panel of Fig.3. In this case, the average of the flow is reasonably described by the model. The introduction of the stochastic version of the model helps to describe the scattering feature of the data, as presented in the right panel of Fig.2. It is observed that the calculated variance is not able to reproduce the scattering of the data close to the transition region. We understand this is due to the interplay between two states (namely, homogeneous free flow and homogeneous congested flow, which are both locally stable states in the deterministic version of the model) of the EoM Eq.(1) and the stochastic noises which trigger the transitions among them. Since our model does not explicitly deal with such temporal evolution, it lies beyond our present scope. On the other hand, one observes that the standard deviation of the data at the congested phase is well described by the model, as it first increases than decreases. As discussed above, stochastic transitions do modify the stability of the corresponding deterministic EoM Eq.(1). The free flow state stretches beyond the point of N_c, meanwhile the homogeneous congested flow phase shrinks and starts only at $N = N_s > N_c$. A small vertical gap consequently appears below the maximum of the flow, and therefore an inverse-λ shape is formed in the right plot of Fig.3. Interestingly enough, we want to emphasize that the above inverse-λ shape would not appear at all, if one only considers stationary traffic states. This is because the stationary traffic state implies the situation where the strength of the random fluctuations is very suppressed; or

in the ideal condition, one considers a traffic system without any stochastic noise where the model reduces to its deterministic version. In the latter case, the stable free flow occurs only within the range $N < N_c$, and the corresponding fundamental diagram restores to being continuous as shown in the left panel of Fig.3. In this context, the discontinuity and the inverse-λ shape in the fundamental diagram is formed dynamically in this model. As the authors understand, this feature of the model is in good agreement of the observed characteristic of the fundamental diagram, and in particular, it is consistent with the feature when the measurements are done for stationary traffic states without much fluctuation.

It is worth mentioning that the above findings in the present work does not contridict the three-phase traffic theory [66, 67] which states that the scattered data on a flow-density plot are caused by stationary states. Since a quasi-stationary solutions of stochastic differential equation stays in the neighborhood of the equilibrium point for a very long period of time, it maintains its average properties (such as velocity and flow) for a reasonably long period of time while involving small temporal oscillations (see the bottom right plot in Fig.4 in Appendix II). On the other hand, small temporal oscillations are indeed observed in realistic traffic states identified to be "sychronized flow" (eg. [79]).

To summarize, in this work we investigate two versions of non-linear transport models for the traffic flow as well as the effect of stochastic transition terms. The two models are closely connected to the well-known "catastrophe model" of traffic flow. For both approaches, a thorough discussion of their stability properties, especially in the deterministic case, is facilitated by the models' simplicity. In our approach, the inverse-λ shape and the associated sudden jump of physical quantities are understood to be associated to the existence of two simultaneous stable traffic flow states and/or to the effect of stochastic transition terms on the stability of the model. In the latter case, the capacity drop is dynamic and it depends on the strength of the stochastic noise terms. The scattering feature of the data is attributed to the noise terms and agrees qualitatively with the data.

ACKNOWLEDGEMENTS

We acknowledge the financial support from Fundação de Amparo à Pesquisa do Estado de São Paulo (FAPESP), Fundação de Amparo à Pesquisa do Estado de Minas Gerais (FAPEMIG), Conselho Nacional de Desenvolvimento Científico e Tecnológico (CNPq), and Coordenação de Aperfeiçoamento de Pessoal de Nível Superior (CAPES).

APPENDIX I: STABILITY OF THE SDE FOR $N < N_c$

Here we show that the free flow solution $x(0,t) \equiv n_1(0,t) = 0$ of the Eq.(1) is *stochastically stable* (Definition 2.1) by using Theorem 2.2 of Chapter 4 of the reference [80]. The outline of the proof is as follows. To show that the solution $x(t) \equiv 0$ is stable for a stochastic equation

$$dx(t) = f(x(t),t)dt + g(x(t),t)dB$$

one needs to find a positive-definite function $V(x,t) \in C^{2,1}(S_h \times [t_0,\infty); R_+)$ such that $LV(x,t) \leq 0$. Here $V(x,t)$ corresponds to the Lyapunov function of an ordinary differential equation, which measures the "distance" of a small perturbation from the equilibrium

solution; and

$$L = \frac{\partial}{\partial t} + \sum_i f_i(x,t)\frac{\partial}{\partial x_i} + \frac{1}{2}\sum_{i,j}[g(x,t)g^T(x,t)]_{i,j}\frac{\partial^2}{\partial x_i \partial x_j}$$

is a differential operator. $LV(x,t)$ bears the interpretation of time derivative of the distance V. Besides, for the theorem to be valid, one needs $f(0,t) = g(0,t) = 0$, which is readily to be satisfied by the equation of n_1

$$dn_1 = \left(-c_1 n_1 + c_2 n_1(N - n_1)\frac{1}{N_{max} - N}\right)dt - \sqrt{c_1 n_1}dB_1 + \sqrt{\frac{c_2 n_1(N - n_1)}{N_{max} - N}}dB_2 \quad (19)$$

Now let us take $V(x,t) = x$. It is straightforward to show that V is indeed positive definite and

$$LV(x,t) = -c_1 x + c_2 x(N - x)\frac{1}{N_{max} - N}$$

It is straightforward to show that the condition $LV \leq 0$ implies $N < N_c$, with N_c defined in Eq.(7).

APPENDIX II: NUMERICAL STUDY OF THE STABILITY OF THE SDE

In this Appendix, we numerically study the stability of the expected value as well as the variance of the free flow and congested flow solutions of Eq.(1) according to their definitions. The equation for free flow is Eq.(19). One may also write down the equation for the congested flow

$$d\tilde{n}_1 = \left(c_1\tilde{n}_1 - c_2\tilde{n}_1(N + \tilde{n}_1)\frac{1}{N_{max} - N}\right)dt - \sqrt{c_1(\tilde{n}_1 + n_g^*)}dB_1 + \sqrt{\frac{c_2(\tilde{n}_1 + n_g^*)(N - (\tilde{n}_1 - n_g^*))}{N_{max} - N}}dB_2$$

where one makes use of $n_1 \to \tilde{n}_1 = n_1 - n^*{}_g$, such that $\tilde{n}_1 = 0$ corresponds to the congested flow solution and the stochastic stablity can be verified according to its definition. We note that the above equation is not symmetric in comparison to Eq.(19), since the former has $\tilde{f}(0,t) = 0$ and $\tilde{g}(0,t) \neq 0$. The parameter space of the system is one-dimensional, therefore it is sufficient to present the numerical results of the evolution of free flow as shown in Fig.4 below.

Fig.4 shows that both the expected value and variance of the free flow is stochastically stable (approaches zero) when $N < N_c$ as proven in Appendix I. However, the range of stable free flow actually reaches beyond N_c. In fact, free flow is stable when $N < N_s$ with $N_s > N_c$. When $N > N_s$, the system evolves towards the equilibrium $n_1 = n_g^*$ (Eq.(5)) and stays in its neighborhood for a very long period of time before it eventually evolves to the absorbing boundary. It is noted that such temporal evolution is stochastic in nature and therefore not periodic, it is known as a quasi-stationary solution according to [77]. Since n_g^* corresponds to the congested flow state in the deterministic "fold catastrophe" model, we therefore identify this solution as the congested flow state. Numerically one finds $k_s = k_c + 15.5 \pm 0.5$.

[1] N. J. Pedersen and et.al., Transp. Res. Cir. **E-C149**, 1 (2011).

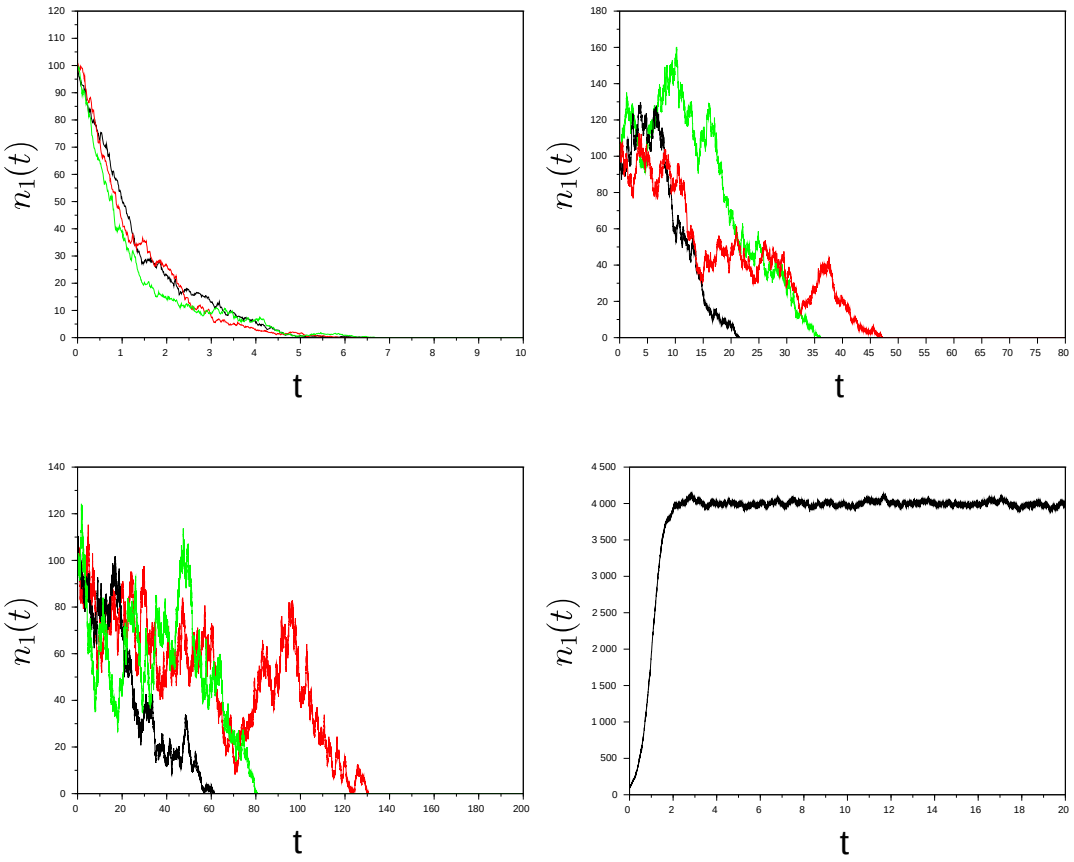

FIG. 4. Numerical study of the stability of the SDE for the free flow and the congested flow. The calculations are carried out using the same parameters of the fit shown in Fig.3, one has $N_c = 2204$. The plots show the temporal evolution of small perturbations ($n_1(0) = 100$) for different road concentrations $k = N/L$. Each plot illustrates (in different colors) several of many numerical simulations carried out. Top left: temporal evolution for small perturbations for the free flow state with $N = 1000 < N_c$; Top right: the same as the top left plot but with $N = N_c$; Bottom left: the same as the top left plot but with $N_c < N = 2214 < N_s = 2360$, all the three plots show that numerically $n_1(t \to +\infty) = 0$, therefore the solution is stochastically stable as long as $N < N_s$; Bottom right: the same as the top left plot but with $N = 5204 > N_s$, it shows that the system evolves to a quasi-stationary state as $n_1 \to n_g^*$.

[2] B. S. Kerner and H. Rehborn, Phys. Rev. **E53**, R4275 (1996).
[3] C. F. Daganzo, Transp. Res. **B36**, 131 (2002).
[4] M. Cassidy, Transp. Res. **B32**, 49 (1998).
[5] L. Edie, Oper. Res. **9**, 66 (1961).
[6] J. S. Drake and J. L. Schofer, H. Res. Rec. **156**, 53 (1967).
[7] H. Payne, Transp. Res. Rec. **971**, 104 (1984).
[8] F. Hall, V. Hurdle, and J. Banks, Transp. Res. Rec. **1365**, 12 (1992).
[9] J. H. Banks, Transp. Res. Rec. **1287**, 20 (1990).
[10] J. H. Banks, Transp. Res. Rec. **1320**, 234 (1991).
[11] K. Hall, F. L.and Agyemang-Duah, Transp. Res. Rec. **1320**, 91 (1991).

[12] D. C. Munoz, J.C., Transp. Sci. **37**, 312 (2003).
[13] M. J. Cassidy and M. Mauch, Transp. Res. **A35**, 143 (2001).
[14] G. Newell, Transp. Res. **B36**, 195 (2002).
[15] C. F. Daganzo, Trans. Res. **B41**, 49 (2007).
[16] S. Blandin, J. Argote, A. M. Bayen, and D. B. Work, Transp. Res. **B52**, 31 (2013).
[17] W.-L. Jin, Q.-J. Gan, and J.-P. Lebacque, Transp. Res. **B81**, 316 (2015).
[18] K. Nagel, P. Wagner, and R. Woesler, Oper. Res. **51**, 681 (2003).
[19] X. Small, Kenneth A.and Chu, Jour. Trans. Econom. Pol. **37**, 319 (2003).
[20] H. Wang, D. Ni, Q.-Y. Chen, and J. Li, Jour. Adv. Trans. **47**, 126 (2013).
[21] J. Li and H. M. Zhang, Transp. Res. Rec. **2260**, 50 (2011).
[22] C. Geroliminis, N.and Daganzo, Transp. Res. **B42**, 759 (2008).
[23] N. Geroliminis and J. Sun, Transp. Res. **B45**, 966 (2011).
[24] J. A. Laval, Transp. Res **B45**, 385 (2011).
[25] B. Coifman, Transp. Res **B68**, 173 (2014).
[26] J. M. D. Castillo and F. G. Benitez, Transp. Res. **B29**, 373 (1995).
[27] M. Treiber and D. Helbing, Phys. Rev. **E68**, 046119 (2003).
[28] J. Li, Q.-Y. Chen, H. Wang, and D. Ni, Transportmetrica **8**, 387 (2012).
[29] B. S. Kerner, *The Physics of Traffic: Empirical Freeway Pattern Features, Engineering Applications, and Theory (Understanding Complex Systems)* (Berlin: Springer, 2004).
[30] P. Nelson and A. Sopasakis, Transp. Res. **B32B**, 589 (1998).
[31] R. Boel and L. Mihaylova, Transp. Res. **B40**, 319 (2006).
[32] S. E. Jabari and H. X. Liu, Transp. Res. **B46**, 156 (2012).
[33] A. Sumalee, R. Zhong, T. Pan, and W. Szeto, Transp. Res. **B45**, 507 (2011).
[34] Y. Wang and M. Papageorgiou, Transp. Res. **B39**, 141 (2005).
[35] P. Wagner, Euro. Phys. J. **B84**, 713 (2011).
[36] P. Huang, L. Kong, and M. Liu, Acta Physica Sinica **50**, 30 (2001).
[37] D. J. Dailey and F. W. Cathey, Research Report **WA-RD 534.1**, 1 (2002).
[38] K. Nagel and M. Schreckenberg, J. Phys. I France **2**, 2221 (1992).
[39] Schadschneider and Schreckenberg, J. Phys. A **26**, L679 (1993).
[40] A. Sopasakis and M. A. Katsoulakis, SIAM Applied Math **66**, 921 (2006).
[41] M. Kanai, K. Nishinari, and T. Tokihiro, Phys. Rev. **E72**, 035102(R) (2005).
[42] A. Yamauchi, J. Tanimoto, A. Hagishima, and H. Sagara, Phys. Rev. **E79**, 036104 (2009).
[43] K. Shigaki, J. Tanimoto, and A. Hagishima, International Journal of Modern Physics **C22**, 1005 (2011).
[44] S. Kokubo, J. Tanimoto, and A. Hagishima, Physica **A390**, 561 (2011).
[45] Y. Wang, M. Papageorgiou, and A. Messmer, Transp. Res. **C14**, 190 (2006).
[46] D. Ngoduy, Transportmetrica **7**, 111 (2011).
[47] W. Brilon, J. Geistefeldt, and M. Regler, Proc. of the 16th International Symposium on Transportation and Traffic Theory , 125 (2005).
[48] J. R. Windover and C. M. J., Transp. Res. **A35**, 881 (2001).
[49] J. A. Laval and C. F. Daganzo, Trans. Res. **B40**, 251 (2006).
[50] B. S. Kerner and P. Konhauser, Phys. Rev. **E48**, R2335 (1993).
[51] M. Bando, K. Hasebe, A. Nakayama, A. Shibata, and Y. Sugiyama, Phys. Rev. E **51**, 1035 (1995).
[52] E. Ben-Naim, P. L. Krapivsky, and S. Redner, Phys. Rev. E **50**, 822 (1994).
[53] T. S. Komatsu and S. ichi Sasa, Phys. Rev. E **52**, 5574 (1995).

[54] M. Treiber, A. Hennecke, and D. Helbing, Phys. Rev. **E62**, 1805 (2000).

[55] V. I. Arnold, *Bifurcation Theory and Catastrophe Theory*, Dynamical Systems Vol. 5, 1 ed. (Springer, 1994).

[56] F. L. Hall, Transp. Res. **A3**, 191 (1987).

[57] B. S. Kerner, *Introduction to modern traffic flow theory and control. The long road to three-phase traffic theory* (Berlin: Springer, 2009).

[58] B. Eisenblatter, L. Santen, A. Schadschneider, and M. Schreckenberg, Phys. Rev. E **57**, 1309 (1998).

[59] J. Tanimoto, *Fundamentals of Evolutionary Game Theory and its Applications* (Springer Japan, 2015).

[60] B. S. Kerner and P. Konhauser, Phys. Rev. **E50**, 54 (1994).

[61] H. Y. Lee, H.-W. Lee, and D. Kim, Phys. Rev. Lett **81**, 1130 (1998).

[62] H. Y. Lee, H.-W. Lee, and D. Kim, Phys. Rev. **E59**, 5101 (1999).

[63] M. Treiber, A. Hennecke, and D. Helbing, Phys. Rev. **E59**, 239 (1999).

[64] D. Helbing, A. Hennecke, and M. Treiber, Phys. Rev. Lett. **82**, 4360 (1999).

[65] C. Daganzo, M. Cassidy, and R. Bertini, Transp. Res. **A33**, 365 (1999).

[66] B. S. Kerner, Physica A **333**, 379440 (2004).

[67] B. S. Kerner and S. L. Klenov, Transp. Res. Rec. **1965**, 70 (2006).

[68] A. F. Siqueira, C. J. T. Peixoto, C. Wu, and W.-L. Qian, Transp. Res. **B87**, 1 (2016), arXiv:1408.2902.

[69] W.-L. Qian, B. Wang, K. Lin, R. F. Machado, and Y. Hama, (2015), arXiv:1508.02768.

[70] W.-L. Qian, R. F. Machado, K. Lin, and A. F. Sequeira, (2016).

[71] W. Sanns, *Catastrophe Theory with Mathematica: A Geometric Approach*, 1 ed. (Der Andere Verlag, 2000).

[72] B. Oksendal, *Stochastic Differential Equations: An Introduction with Applications*, 6 ed. (Springer, 2010).

[73] L. Arnold, H. Crauel, and V. Wihstutz, SIAM J. Control Optim **21**, 451 (1983).

[74] A. A. Kwiecinska, Stoc. Proc. Appl. **79**, 179 (1999).

[75] X. Mao, Stoc. Proc. Appl. **79**, 45 (1999).

[76] M. Scheutzow, Stoc. Ana. Appl. **11**, 97 (1993).

[77] J. Grasman and O. A. van Herwaarden, *Asymptotic Methods for the Fokker-Planck Equation and the Exit Problem in Applications*, 1 ed. (Springer, 1999).

[78] W.-L. Jin, Transp. Res. Rec. **2188**, 55 (2010).

[79] B. S. Kerner, Phys. Rev. Lett. **81**, 3797 (1998).

[80] X. Mao, *Stochastic Differential Equations and Applications*, 2 ed. (Woodhead Publishing, 2007).